



Transcriptome Assembly and Profiling of *Candida auris* Reveals Novel Insights into Biofilm-Mediated Resistance

Ryan Kean,^{a,b} Christopher Delaney,^a Leighann Sherry,^a Andrew Borman,^c Elizabeth M. Johnson,^c Malcolm D. Richardson,^d Riina Rautemaa-Richardson,^d Craig Williams,^{b,e} Gordon Ramage^{a,e}

^aOral Sciences Research Group, School of Medicine, Dentistry and Nursing, College of Medical, Veterinary and Life Sciences, University of Glasgow, Glasgow, United Kingdom

^bInstitute of Healthcare, Policy and Practise, University of the West of Scotland, Paisley, United Kingdom

^cNational Mycology Reference Laboratory, Public Health England South-West, Bristol, United Kingdom

^dMycology Reference Centre Manchester, University Hospital of South Manchester & University of Manchester, Manchester Academic Health Sciences Centre, Faculty of Biology, Medicine and Health, Division of Infection, Immunity and Respiratory Medicine, Manchester, United Kingdom

^eESCMID Study Group for Biofilms (ESGB)‡

ABSTRACT *Candida auris* has emerged as a significant global nosocomial pathogen. This is primarily due to its antifungal resistance profile but also its capacity to form adherent biofilm communities on a range of clinically important substrates. While we have a comprehensive understanding of how other *Candida* species resist and respond to antifungal challenge within the sessile phenotype, our current understanding of *C. auris* biofilm-mediated resistance is lacking. In this study, we are the first to perform transcriptomic analysis of temporally developing *C. auris* biofilms, which were shown to exhibit phase- and antifungal class-dependent resistance profiles. A *de novo* transcriptome assembly was performed, where sequenced sample reads were assembled into an ~11.5-Mb transcriptome consisting of 5,848 genes. Differential expression (DE) analysis demonstrated that 791 and 464 genes were up-regulated in biofilm formation and planktonic cells, respectively, with a minimum 2-fold change. Adhesin-related glycosylphosphatidylinositol (GPI)-anchored cell wall genes were upregulated at all time points of biofilm formation. As the biofilm developed into intermediate and mature stages, a number of genes encoding efflux pumps were upregulated, including ATP-binding cassette (ABC) and major facilitator superfamily (MFS) transporters. When we assessed efflux pump activity biochemically, biofilm efflux was greater than that of planktonic cells at 12 and 24 h. When these were inhibited, fluconazole sensitivity was enhanced 4- to 16-fold. This study demonstrates the importance of efflux-mediated resistance within complex *C. auris* communities and may explain the resistance of *C. auris* to a range of antimicrobial agents within the hospital environment.

IMPORTANCE Fungal infections represent an important cause of human morbidity and mortality, particularly if the fungi adhere to and grow on both biological and inanimate surfaces as communities of cells (biofilms). Recently, a previously unrecognized yeast, *Candida auris*, has emerged globally that has led to widespread concern due to the difficulty in treating it with existing antifungal agents. Alarmingly, it is also able to grow as a biofilm that is highly resistant to antifungal agents, yet we are unclear about how it does this. Here, we used a molecular approach to investigate the genes that are important in causing the cells to be resistant within the biofilm. The work provides significant insights into the importance of efflux pumps, which actively pump out toxic antifungal drugs and therefore enhance fungal survival within a variety of harsh environments.

KEYWORDS *Candida*, antifungal resistance, biofilms, efflux pumps, gene expression

Received 20 June 2018 Accepted 21 June 2018 Published 11 July 2018

Citation Kean R, Delaney C, Sherry L, Borman A, Johnson EM, Richardson MD, Rautemaa-Richardson R, Williams C, Ramage G. 2018. Transcriptome assembly and profiling of *Candida auris* reveals novel insights into biofilm-mediated resistance. mSphere 3:e00334-18. <https://doi.org/10.1128/mSphere.00334-18>.

Editor Aaron P. Mitchell, Carnegie Mellon University

Copyright © 2018 Kean et al. This is an open-access article distributed under the terms of the [Creative Commons Attribution 4.0 International license](https://creativecommons.org/licenses/by/4.0/).

Address correspondence to Gordon Ramage, Gordon.Ramage@glasgow.ac.uk.

R.K. and C.D. contributed equally to this work.

‡ For this virtual institution, see https://www.escmid.org/research_projects/study_groups/biofilms/.

 *Candida auris* biofilms display conserved characteristics of other *Candida* species biofilms, with efflux-mediated resistance an important mechanism of temporal resistance. @ramage_gordon

Fungal infections affect in excess of a billion people, resulting in approximately 11.5 million life-threatening infections and more than 1.5 million deaths annually (1). *Candida auris* is an emerging fungal pathogen that has attracted considerable attention because of its ability to cause infections that are difficult both to diagnose and to treat (2). It has been responsible for a number of nosocomial outbreaks worldwide through its ability to persistently colonize and be transmitted between patients and the environment (3–6). Despite the unprecedented global emergence of this organism, relatively little is known about the molecular basis of its pathogenicity and antifungal resistance phenotype. The resistance profile is well documented, with >90% of isolates intrinsically resistant to fluconazole. Resistance to other azoles, polyenes, and echinocandins has also been reported (4). Alarming, 41% of isolates have been shown to be multidrug resistant, with 4% demonstrating pan-drug resistance (4). Hot spot mutations in *ERG11* and *FKS1* have been identified as resistance mechanisms in azole- and echinocandin-resistant strains, respectively (7, 8).

Candida biofilms represent an important clinical entity associated with adaptive resistance to many antifungals and are linked to excess morbidity and mortality (9–11). Although *Candida albicans* is regarded as the primary biofilm-forming pathogen within the genus, there are increasing interest in and evidence for non-*Candida albicans*-species biofilms (12, 13), particularly those of *C. auris*. Clinically, *C. auris* has been isolated from a number of sites, including wounds, line tips, and catheters, suggestive of the organism existing within a biofilm lifestyle in the host (14, 15). We recently described the ability of *C. auris* to form antifungal-resistant biofilms, against all 3 main classes of antifungals (16), and yet the mechanisms underlying this phenotype remain unknown. The speed of discovery in this emerging pathogen has certainly been hindered by the lack of robust sequence information. Initial sequencing efforts provided a draft *C. auris* genome; however, these reads were poorly aligned to other *Candida* spp. and inconsistently annotated (17). More recently, complete and functionally annotated genome assemblies have been created, allowing the analysis of the functional capacity of the genome to be studied under clinically relevant conditions (18). Biofilm-associated resistance is a complex and multifaceted phenomenon that has been described in a number of fungal pathogens. Various resistance mechanisms exist, predominately associated with the extracellular matrix (ECM), overexpression of drug targets, and efflux pumps (19). Given the lack of understanding of biofilm formation and resistance mechanisms in *C. auris*, we therefore aimed to investigate these mechanisms using a transcriptomics approach.

RESULTS

***Candida auris* biofilms exhibit temporal antifungal resistance.** Mature *Candida auris* biofilms have been shown to be resistant to antifungals that are readily active against their planktonic equivalents (16). We therefore investigated the temporal effect of biofilm formation on the susceptibility to all three major classes of antifungals. As demonstrated in Fig. 1A, the maturation of *C. auris* biofilms was shown to correlate with decreased susceptibility to each antifungal agent. When assessed planktonically, the median MIC for the four isolates of miconazole was 1 $\mu\text{g/ml}$, that of micafungin was <0.25 $\mu\text{g/ml}$, and that of amphotericin B was 0.5 $\mu\text{g/ml}$ (range, 0.125 to 0.5 $\mu\text{g/ml}$). After 4 h of biofilm development, no increases in resistance were observed against micafungin (MIC, <0.25 $\mu\text{g/ml}$); however, the median MIC increased 16-fold to 16 $\mu\text{g/ml}$ (range, 16 to 32 $\mu\text{g/ml}$) for miconazole and 4-fold to 2 $\mu\text{g/ml}$ for amphotericin B (range, 1 to 4 $\mu\text{g/ml}$). As the biofilm matured to 12 h of growth, 2-fold increases in median MIC were shown for miconazole (range, 16 to 64 $\mu\text{g/ml}$) and amphotericin B (range, 2 to 4 $\mu\text{g/ml}$). Interestingly, the MIC was shown to significantly increase for micafungin (range, 1 to >128 $\mu\text{g/ml}$) after 12 h. After 24 h, no further increase in MIC was observed for amphotericin B. However, both miconazole and micafungin MICs were increased 2-fold to 64 $\mu\text{g/ml}$ and >128 $\mu\text{g/ml}$, respectively.

***Candida auris* transcriptome assembly.** Given the temporal patterns of biofilm-associated resistance, we undertook a transcriptional profiling approach to understand

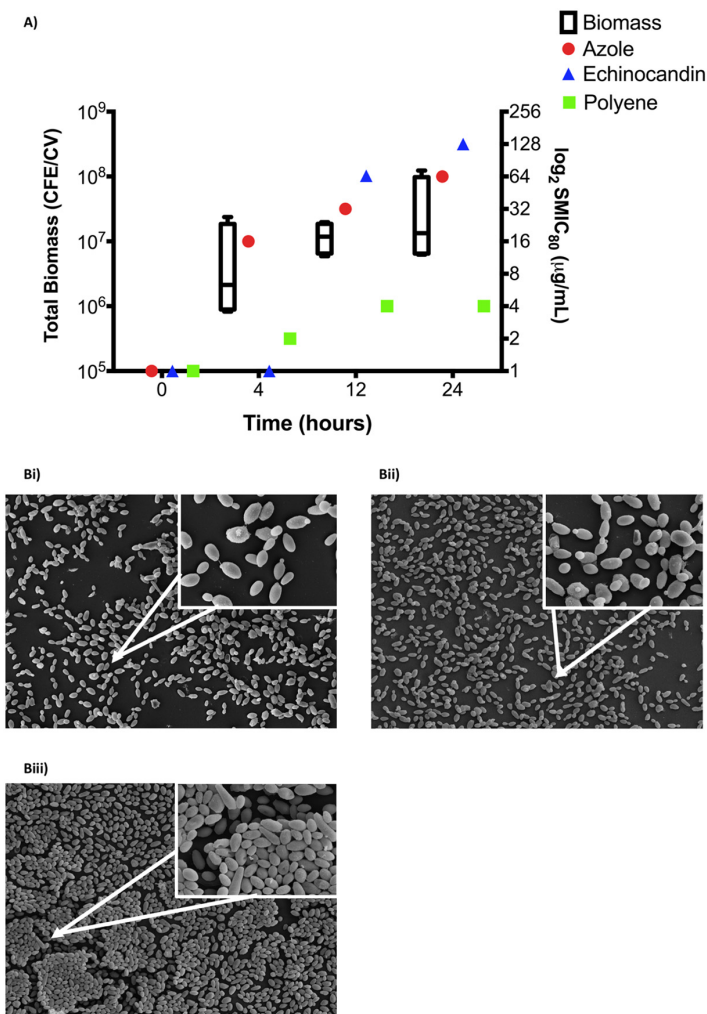


FIG 1 *Candida auris* biofilm development correlates with increased antifungal tolerance. *Candida auris* biofilms were standardized at 1×10^6 CFU/ml and grown for 4, 12, and 24 h. Biofilm biomass was then quantified using the crystal violet assay, with the composition of biofilm cells enumerated using qPCR and represented by a box-and-whisker plot as the total biomass of four *C. auris* isolates (A, left y axis). Planktonic susceptibility testing was performed against serially diluted miconazole, micafungin, and amphotericin B concentrations using the CLSI guidelines, with biofilm susceptibility testing performed using the XTT assay and with median MIC values plotted (A, right y axis). In addition, biofilms were grown, fixed, and processed for SEM before imaging using a JEOL-JSM-6400 scanning electron microscope. Micrographs represent lower magnification ($\times 1,000$) and higher magnification (inset, $\times 5,000$) of biofilms grown for 4 h (Bi), 12 h (Bii), and 24 h (Biii).

the mechanisms governing antifungal biofilm resistance (Fig. 2). Sequencing of samples using Illumina HiSeq produced around 414 million single-end reads of 50-bp length. Following processing, the number of reads was reduced by 3 million through trimming and quality control stages. All sequenced sample reads were then assembled into an ~11.5-Mb transcriptome which consisted of 5,889 identified Trinity transcripts and 5,848 genes based on the longest isoform of transcripts. At least half of the assembled sequenced bases were found on contigs of a length of 3,488 bp (N_{50}) (Table 1). The completeness and quality of the *C. auris* transcriptome were assessed with BUSCO (Benchmarking Universal Single-Copy Orthologs) against Ascomycota (94%), Saccharomyceta (91.4%), and Saccharomycetales (91.7%) gene sets. Very small percentages of duplicate, fragmented, and missing genes were observed in each of the gene sets (Table 2).

Identification by sequence homology searches with BLASTx function yielded annotation of 54% of Trinity transcripts and 54% of unique “genes.” Identification of protein

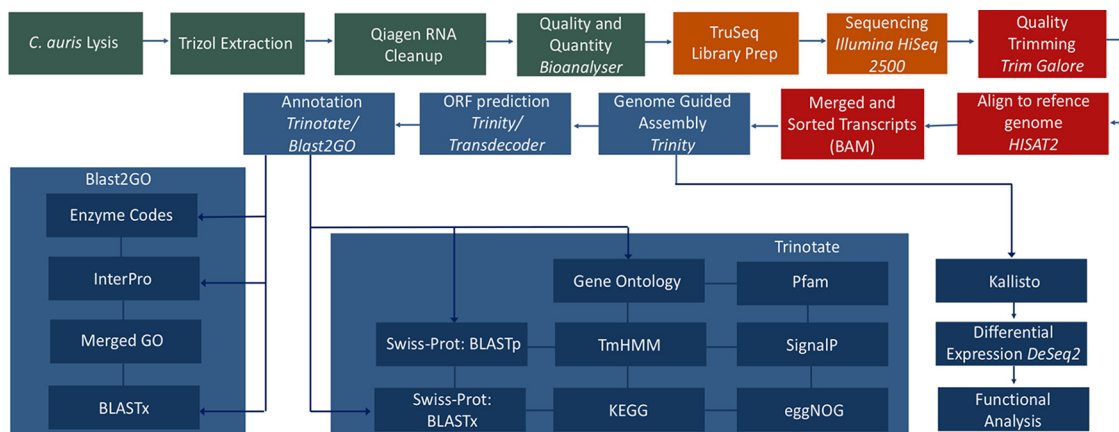


FIG 2 Bioinformatic pipeline for *Candida auris* transcriptome assembly, annotation, and analysis.

sequences with BLASTp, against TransDecoder-identified open reading frames (ORFs) and potential coding sequences, gave functional annotation matches with 51% of the transcripts and 41% of unique “genes” (Table 1). The presence of known signal peptides, functional protein domains, and protein topology was discerned by searches against the SignalP and TMHMM databases, respectively. Of the predicted proteins, 202 sequences were predicted to have signal peptides and 701 transmembrane protein topologies were predicted.

Additional annotation was performed via the software BLAST2GO, which obtains BLAST hits that are used to retrieve and map gene ontology (GO) and KEGG terms. It also utilizes InterProScan, which acquires functional annotation of protein sequences

TABLE 1 Summarized statistics for transcriptome assembly of *Candida auris*, alignment rate of raw reads to transcriptome, and summary of Trinotate functional annotation

Category	Value
No. of reads	
Total	414,364,539
After trimming	411,626,529
Total no. of assembled bases	11,593,681
GC content, %	45.35
Total no. by Trinity	
“Genes”	5,848
“Transcripts”	5,889
Contig (bp)	
N ₅₀	3,488
Median	1,308
Avg	1,983
No. of reads aligned (%)	
1 time	393,124,946 (95.51)
>1 time	9,368,727 (2.28)
Overall	402,493,673 (97.78)
Functional annotation, no. of transcripts	
Swiss-Prot matches, BLASTx	3,200
Swiss-Prot unique proteins, BLASTx	3,176
Swiss-Prot matches, BLASTp	3,041
Swiss-Prot unique proteins, BLASTp	3,019
TMHMM	701
SignalP	202
Gene Ontology	3,085
KEGG	2,889

TABLE 2 Assessment of *Candida auris* transcriptome assembly by Benchmarking Universal Single-Copy Orthologs (BUSCO)

% genes	Ascomycota	Saccharomyceta	Saccharomycetales
Complete	94	91.4	91.7
Complete single copy	93.4	90.5	90.9
Complete duplicated	0.6	0.9	0.8
Fragmented	3.4	4.8	4.6
Missing	2.6	3.8	3.7
Total no. of genes	1,315	1,759	1,711

from EBI's InterPro databases (<https://www.ebi.ac.uk/interpro/>). These databases are a consortium of online databases that include PANTHER, Pfam, and SUPERFAMILY (20). Both the Trinotate and BLAST2GO annotation files are supplied as Data Set S1 in the supplemental material.

BLAST2GO searches were performed with a fungus taxonomical filter, which annotated 1,157 genes with BLAST and an additional 4,365 genes from the InterPro databases. InterPro and BLAST-derived GO terms were merged to give a total of 9,504 GO annotations assigned to 2,479 genes. These annotations were distributed among three main GO categories, biological process (3,633, 38%), cellular component (3,116, 33%), and molecular function (2,755, 29%) (Fig. S1). InterProScan was able to classify Trinity transcripts according to superfamilies based on known structures. The best-represented superfamilies were the P-loop-containing nucleoside triphosphate hydrolyase (236 genes), the major facilitator superfamily (MFS) (113 genes), Armadillo-type fold (102 genes), and protein kinase-like superfamily (90 genes) (Fig. S2). From annotation against the available databases, there were 6 major enzyme classes represented, which included hydrolyases (290 genes), transferases (150 genes), oxidoreductases (88 genes), ligases (21 genes), lyases (22 genes), and isomerases (15 genes) (Fig. S3).

DE and functional annotation of *C. auris* biofilms. Differential expression (DE) analysis was performed to investigate the transcriptional changes observed with biofilm development. Multivariate analysis by principal-component analysis (PCA) demonstrates variance between the different time points; 0 h shows the greatest variance from the other biofilm time points. In addition, there is also some variance between biofilms at 4, 12, and 24 h (Fig. 3A). DE analysis demonstrated that 791 and 464 genes were upregulated in biofilm formation and planktonic cells, respectively, with a minimum 2-fold change (Fig. 3A). Phase-dependent differential expression of these upregulated genes is illustrated in the Venn diagram in Fig. 3B, with the downregulated genes shown in Fig. 3C; individual genes are described in Data Set S2. Of these biofilm-upregulated genes, selected genes involved in antifungal resistance and biofilm-associated mechanisms are listed in Table 3. Glycosylphosphatidylinositol (GPI)-anchored cell wall genes, including *IFF4*, *CSA1*, *PGA26*, and *PGA52*, were upregulated at all time points of biofilm formation, highlighting their potential role within cellular adhesion (Table 3). Two further adhesins, *HYR3* and *ALS5*, were also shown to be upregulated but only in mature biofilms (Table 3). As the biofilm developed into intermediate and mature stages, a number of genes encoding efflux pumps were upregulated, including *RDC3*, *SNQ2*, *CDR1*, and *YHD3*. In addition, *MDR1* was shown to be upregulated at the 24-h time point (Table 3). To understand the functional processes related to differentially expressed genes, a cutoff of 2-fold upregulation (adjusted *P* value of <0.05) was used for gene ontology (GO) analysis comparing planktonic cells to 24-h biofilms. The 278 differentially expressed genes were assigned to 28 GO terms with an overenrichment *P* value of <0.05, comprising 13 biological processes, 9 cellular components, and 6 molecular functions, and contained a number of differentially expressed functional categories (Fig. 4A). Included within these GO terms were transmembrane transport, within which several ATP-binding cassette (ABC) and major facilitator superfamily (MFS) transporters were highly upregulated in *C. auris* biofilms (Fig. 4B).

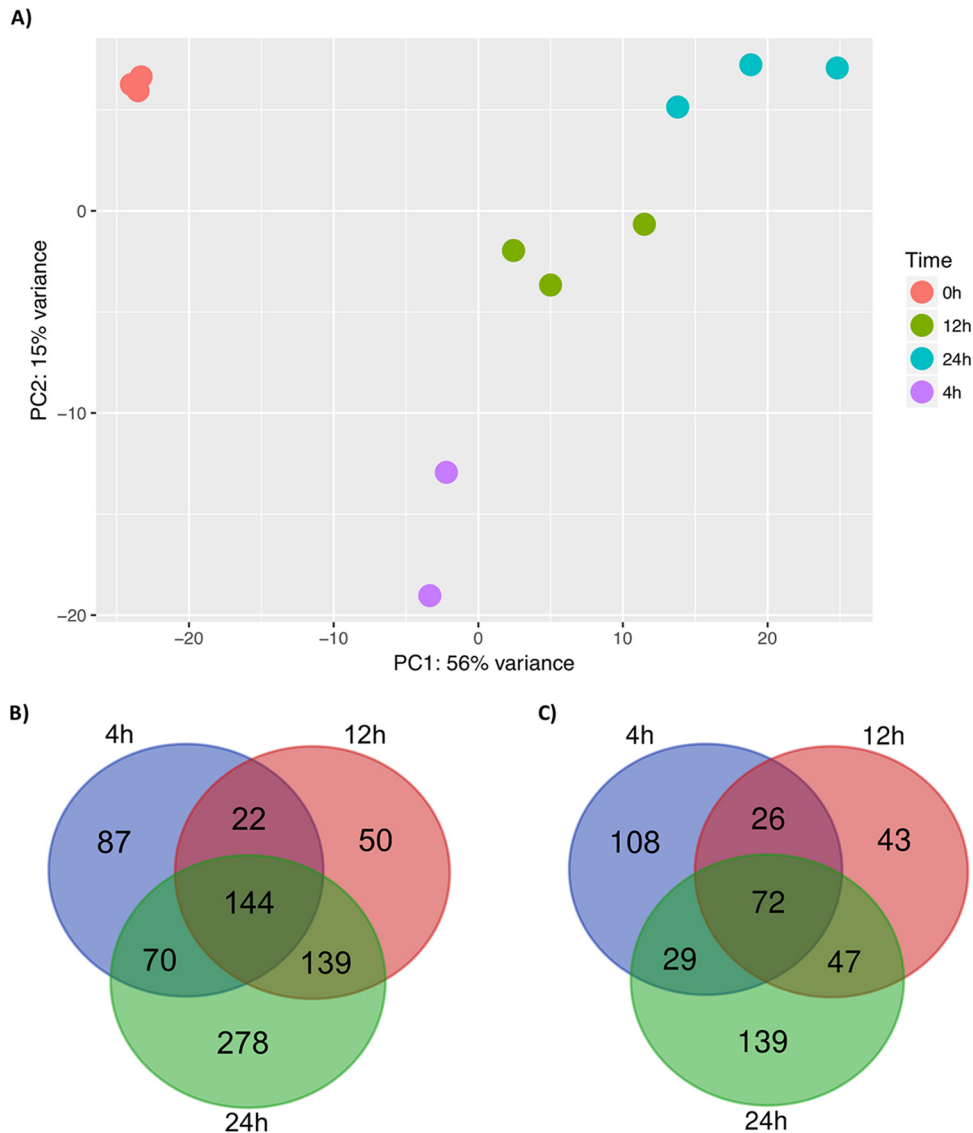


FIG 3 Quality control and differential expression analysis of *C. auris* biofilms. Principal-component analysis displays the largest variance along PC1 (56%) and the second largest variance between samples along PC2 (15%) (A). Venn diagrams of the genes upregulated (B) and downregulated (C) in biofilm time points (4, 12, and 24 h) compared to 0 h.

Efflux pumps play a primary role in antifungal resistance in *C. auris* biofilms.

Transcriptional analysis and function annotation revealed a significant upregulation of a number of drug efflux pumps, from both ABC and MFS transporters. To confirm the role of these membrane proteins within biofilms, we assessed efflux pump activity. Both 12- and 24-h biofilms exhibited increased efflux compared to planktonic cells, with 4-h biofilms below the detectable limit of the assay. Efflux from 12-h biofilms was 2.21-fold ($P < 0.05$) greater than that from planktonic cells, with a 2.38-fold increase shown in 24-h biofilms ($P < 0.005$). No statistical differences were observed between 12- and 24 h-biofilms (Fig. 5). Interestingly, efflux pump activity is shown to be constitutively expressed within biofilms, with no induction observed in response to azole antifungals (Fig. S4).

Given the increased activity of efflux pumps in biofilms, we then assessed the contribution of these transporters to fluconazole sensitivity (Table 4). When biofilms were incubated for 12 h in the presence of fluconazole, the sessile MIC₅₀ (SMIC₅₀) ranged between 32 and >128 $\mu\text{g/ml}$. However, when also grown in the presence of

TABLE 3 Upregulated biofilm- and resistance-associated genes

Gene identifier	Function	Fold change compared to planktonic cells (log ₂)		
		4 h	12 h	24 h
<i>IFF4</i>	Adhesion	2.29	5.01	3.62
<i>PGA26</i>	Adhesion	2.02	3.90	2.55
<i>PGA52</i>	Adhesion	2.22	2.38	2.42
<i>CSA1</i>	Adhesion	3.87	6.47	6.43
<i>PGA7</i>	Adhesion		3.94	4.82
<i>HYR3</i>	Adhesion			2.06
<i>ALS5</i>	Adhesion			3.82
<i>RDC3</i>	Efflux pump		4.29	3.91
<i>SNQ2</i>	Efflux pump		2.63	3.42
<i>CDR1</i>	Efflux pump		2.30	3.19
<i>YHD3</i>	Efflux pump		2.14	2.15
<i>MDR1</i>	Efflux pump			2.3
<i>KRE6</i>	Extracellular matrix		3.92	3.09
<i>EXG</i>	Extracellular matrix		2.69	2.26
<i>SAP5</i>	Hydrolytic enzyme			2.19
<i>PLB3</i>	Hydrolytic enzyme			2.13

fluconazole and an efflux pump inhibitor (EPI), the SMIC₅₀ ranged between 2 and 16 $\mu\text{g/ml}$ for all isolates, ranging from a 4- to 16-fold increase in susceptibility. The same trend was observed for 24-h biofilms, with the SMIC₅₀ range between 64 and >128 $\mu\text{g/ml}$ for fluconazole-only treatment, with 2- to 8-fold reductions observed with coinubation with the EPI (SMIC₅₀, 8 to 64 $\mu\text{g/ml}$).

DISCUSSION

The rapid and simultaneous emergence of the pathogenic yeast *C. auris*, combined with its reported recalcitrance to all three major classes of antifungals, has led to a concerted response by the medical mycology community to understand and define the mechanisms underpinning its pathogenicity and resistance. Although preliminary investigations have investigated genetic point mutations promoting resistance (7, 8), as well as a number of efflux pumps identified within its genome (17, 18), there are still substantial gaps remaining in our understanding. Moreover, irrespective of these defined chromosomally derived resistance characteristics, adaptive resistance mechanisms associated with environmental stressors are likely to be a key contributor to its success as a pathogen in both the host and the environment. We have recently reported how *C. auris* exhibits enhanced pathogenicity and resistance, both *in vitro* and *in vivo*, and that the biofilm phenotype is instrumental in its lifestyle (14, 16, 21, 22), and moreover, in its ability to survive and persist in the nosocomial environment, increasing the probability of causing outbreaks. We have recently reported that adherent *C. auris* cells display substrate-dependent susceptibility to clinically relevant concentrations of hospital disinfectants (22) and that these biofilms were shown to be resistant to chlorhexidine and hydrogen peroxide, displaying a less susceptible phenotype than *C. albicans* and *Candida glabrata* (21). Here, we report for the first time that efflux-based resistance mechanisms play an important role in biofilm-mediated resistance in *C. auris* and that conserved biofilm-related genes are temporally observed, as illustrated in Fig. 6.

To investigate this, we undertook an RNA sequencing-based approach for the analysis of *C. auris* biofilm development, as well as profiling genes associated with resistance and virulence mechanisms. Assembly of the transcriptome using Trinity software has allowed us to construct a specific reference for our samples of interest. Additionally, annotation via numerous methods has allowed for an in-depth functional characterization of the organism. Annotation of homologs, predicted protein domains, and gene ontological classifications further enhances our ability to interpret mechanisms that differentiate *C. auris* under different conditions. This annotated transcrip-

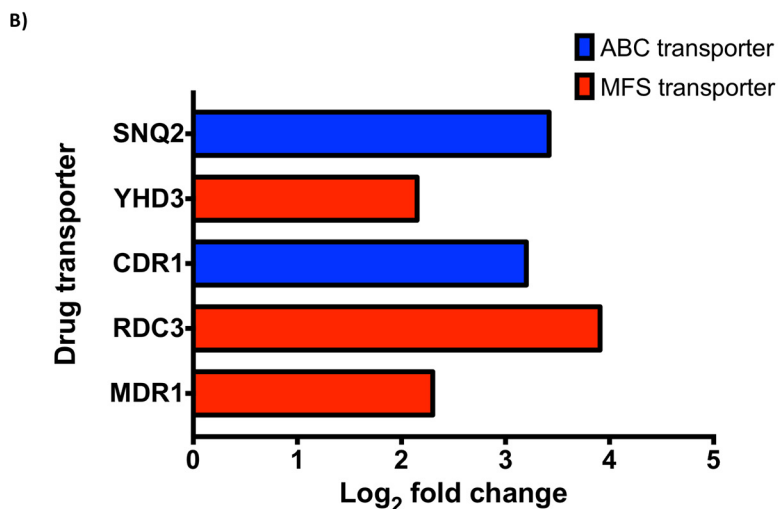
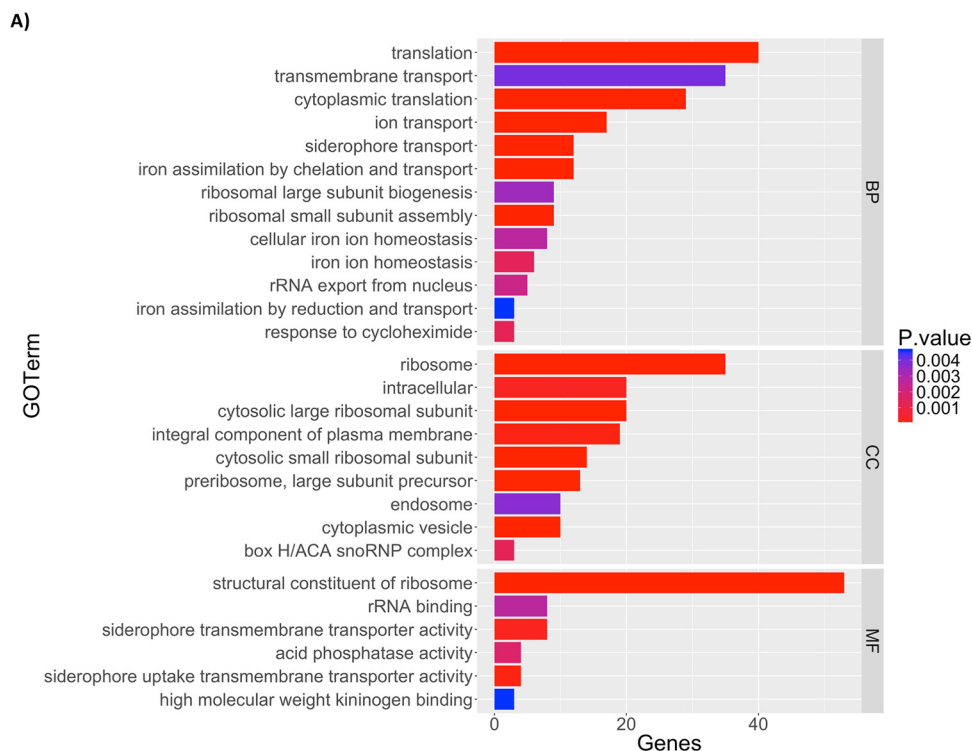


FIG 4 Functional annotation of differentially expressed genes reveals upregulation of drug transporters. Gene distribution of significantly upregulated *C. auris* genes in 24-h biofilms relative to planktonic cells, grouped into biological process (BP), cellular component (CC), and metabolic function (MF) gene ontology categories (A). Log₂ fold change of upregulated ABC and MFS drug transporters within 24-h biofilms (B). All GO terms have a *P* value of <0.05 based upon the GOSep hypergeometric distribution test.

tome has been highly instrumental in expression analysis and elucidation of virulence mechanisms of *C. auris* in this and forthcoming studies.

The initiation of biofilm formation depends on an initial adherence phase of colonization of a specific surface before subsequent proliferation to promote disease. A number of GPI-linked cell wall proteins were upregulated at the early biofilm time point, highlighting their role in the initial adherence stage. In *C. albicans*, IFF4 and CSA1 have been shown to be involved in adherence to both mucosal and abiotic substrates, as well as cell-cell cohesion (23–25). Transcriptional studies from Fox et al. identified IFF4 as a member of a group of 10 adhesion genes that are induced at the later stages

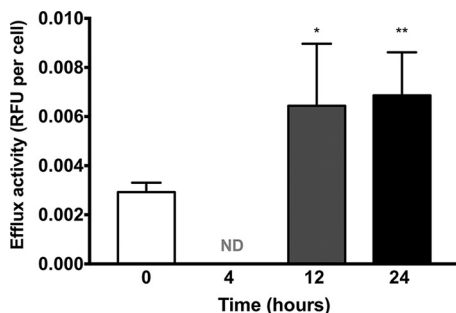


FIG 5 Efflux pump activity is increased in *Candida auris* biofilms. *Candida auris* biofilms were grown for 4, 12, and 24 h in black-bottomed 96-well plates. In addition, planktonic cells were standardized to 5×10^7 cells/ml, all cells were incubated with 100 $\mu\text{g/ml}$ of Ala-Nap, and fluorescence measurements were read at 30-s intervals over 60 min (excitation, 355 nm; emission, 460 nm). Data represent the mean + standard deviation of 4 isolates repeated on 3 independent occasions. Data presented are relative fluorescence units (RFU) normalized per individual cell. *, $P < 0.05$; **, $P < 0.01$; ND, not detectable.

of biofilm formation and hypothesized its role in mediating cell-cell contact (26). Interestingly, an *iff4Δ* null mutant displayed decreased adhesion at an early stage of biofilm formation, as well as attenuated virulence (27). Both studies collectively highlight its function throughout biofilm formation.

In *C. albicans*, members of the agglutinin-like sequence (ALS) proteins play a key role in the adherence of the organism, predominantly through *ALS3* (28, 29). A recent study identified that members of this cell wall protein family detected in *C. albicans* are not found in *C. auris* (18). Our analysis revealed that orthologs of only two members, *ALS1* and *ALS5*, were represented within the *C. auris* transcriptome, with the latter upregulated within mature biofilms. Further examination of cell wall protein families by Muñoz et al. failed to reveal any highly expanded families (18). It is therefore likely that a less reliant ALS-dependent adherence mechanism exists for *C. auris*. Moreover, the gene encoding candidapepsin-5, commonly known as *SAP5* in *C. albicans*, was shown to be upregulated in mature biofilms. This protease is predominantly associated with its role in invasive infection (30). Indeed, studies have identified its increased expression in biofilm-associated infections (31), with *sap5Δ/Δ* strains demonstrating a less adherent phenotype, therefore highlighting its potential as a promising biofilm biomarker (32).

One of the most defining characteristics of biofilms is their recalcitrance to antimicrobial agents. As described in other *Candida* species, biofilm-associated drug resistance comprises a number of different mechanisms that coordinate with one another through the various phases of biofilm development (33). An underlying mechanism across *Candida* spp. is the upregulation of efflux pumps within biofilm-associated cells (34–36). Planktonically, *C. auris* isolates displayed up to 15-fold-higher ABC transporter activity than *C. glabrata* isolates (15), highlighting a potential intrinsic azole resistance mechanism. Ramage et al. demonstrated that expression of *CDR1* and *MDR1* was increased within mature *C. albicans* biofilms compared to their planktonically grown equivalents, and yet deletion of these genes had no effect on the susceptibility of mature biofilms (37). Indeed, temporal efflux pump analysis revealed that efflux pump

TABLE 4 Inhibition of efflux pumps increases azole susceptibility

Isolate no.	Fluconazole SMIC ₅₀ ($\mu\text{g/ml}$) at time:					
	12 h			24 h		
	With EPI ^a	Without EPI	Fold change	With EPI	Without EPI	Fold change
NCPF8971	16	64	4	16	>128	≥ 8
NCPF8973	2	32	16	8	64	8
NCPF8984	16	>128	≥ 8	64	>128	≥ 2
NCPF8990	8	32	4	16	64	4

^aEPI, efflux pump inhibitor.

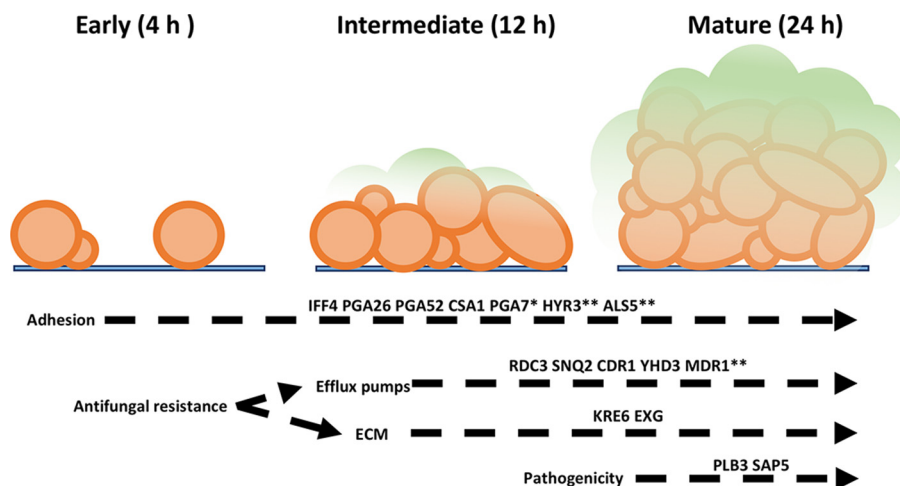


FIG 6 Formation and development of *Candida auris* biofilms. Schematic representation of the transcriptional mediators of the three main stages of *C. auris* biofilm development: adherence of yeast cells to surface (early phase), proliferation (intermediate phase), and maturation into a structured biofilm (mature phase).

mutants were more susceptible to fluconazole treatment than their parental strain at early phases of biofilm development (36), as also shown in other fungal pathogens, such as *Aspergillus fumigatus* (38). Our own temporal analysis of *C. auris* biofilms revealed that efflux pumps were upregulated at intermediate and mature phases of development, unlike other species, though they did not appear to be inducible following azole exposure. This is in contrast to analysis of *C. glabrata* biofilms exposed to azole treatment, where upregulation of genes encoding ABC transporters was observed (35). Muñoz et al. recently analyzed the transcriptional profile of planktonic *C. auris* in response to azole and polyene antifungals (18). After exposure of a resistant *C. auris* strain to amphotericin B, almost 40 genes were shown to be differentially expressed. These included genes involved in iron transport that have previously been described in *C. albicans* to be involved in its response to amphotericin B (39). Three of these genes (*SIT1*, *PGA7*, and *RBT5*) were shown to overlap within our own biofilm data set, indicating that these may play an additional role in our observed polyene resistance.

A further key mechanism of *Candida* biofilm resistance is the formation of the ECM, which functions to provide stability and sequestration of drugs from the biofilm, as well as protection from environmental stressors (40). Recent studies have now identified that various *Candida* spp. conserve a constitutive polysaccharide backbone that functions to impede antifungal delivery, and yet the composition of the ECM varies between species (41, 42). Although its composition remains unknown, it could be hypothesized that *C. auris* ECM would be similar to that of *C. glabrata*, given the yeast cell biofilm phenotype. Temporal analysis has shown that the formation of the ECM is time dependent and associated with intermediate and maturation phases of biofilm formation (43). Our data suggest that this is similar in *C. auris*, with increased expression of *KRE6* and *EXG*, a glucan-1,3-beta-glucosidase and a close ortholog of *XOG1* in *C. albicans*, respectively, two genes involved in matrix formation (44, 45).

Given the alarming global emergence of antifungal resistance, the requirement for new antifungals is pivotal (46). Drug efficacy and development have plateaued in recent years, yet an encouraging number of molecules remain within the antifungal pipeline (47, 48). Several studies have assessed the positive efficacy of novel pipeline compounds, including APX001, CD101, SCY078, and ceragenins, against *C. auris* (49–52), which may widen the spectrum of active agents against emerging resistant species. These active agents are both expansions of current drug targets, such as 1,3- β -glucan synthase inhibitors (CD101 and SCY078), and novel targets, such as GPI protein inhibitors (APX001). All of these compounds demonstrated significant *in vitro* activity against planktonic forms of *C. auris*, with APX001 also demonstrating enhanced *in vivo*

efficacy compared to anidulafungin (51, 53). Although these preliminary data are very promising, there are limited studies evaluating their effect against sessile *C. auris*. The 1,3- β -glucan synthase inhibitor SCY078 was shown to significantly reduce biofilm thickness and metabolic activity after a prolonged 48-h exposure (54). Furthermore, the CSA-44 and CSA-131 ceragenins, a class of antimicrobial peptides, also demonstrated antibiofilm activity, although the concentrations needed were 4- to 64-fold greater than the planktonically active equivalent (52). APX001 is a first-in-class compound that acts by blocking GPI synthesis through inhibition of the GPI-anchored cell wall transfer protein 1 (Gwt1). Although no such studies have been performed, perhaps then APX001 is the most attractive antibiofilm target, given our identified function of GPI-anchored proteins in *C. auris* biofilm formation.

Given that we can now genetically manipulate this pathogenic yeast (55, 56), future work analyzing the functional roles and processes of specific genes and proteins will further enhance our understanding of biofilm-associated pathogenicity and resistance. Unraveling the key factors that regulate the transcriptional network that exists for *C. auris*, similar to those studies in *C. albicans* and *Candida parapsilosis* (26, 57), may provide translational insights into novel avenues for therapeutic targets for biofilm-associated infections. We have shown that efflux pumps are important during biofilm development, and this may explain why this seemingly innocuous yeast is able to survive, persist, and cause continued problems within the hospital setting.

MATERIALS AND METHODS

Microbial growth and standardization. Four *C. auris* clinical isolates were used throughout this study (NCPF8971, NCPF8973, NCPF8984, and NCPF8990) (58). Isolates were stored in Microbank vials at -80°C prior to use, before they were subcultured onto Sabouraud dextrose agar (SAB [Sigma, Dorset, United Kingdom]) and incubated at 30°C for 48 h. Isolates were propagated overnight in yeast peptone dextrose (YPD) medium (Sigma, Dorset, United Kingdom), before washing with centrifugation as previously described (59). Cells were then standardized to 1×10^6 cells/ml in RPMI 1640 medium, and biofilms were grown in microtiter plates, 75-cm² tissue culture flasks, or Thermanox coverslips for 4, 12, and 24 h at 37°C .

Characterization of biofilm formation. Isolates were standardized as described above and grown for 4, 12, and 24 h at 37°C . Following growth, biofilms were washed with phosphate-buffered saline (PBS; Sigma, Dorset, United Kingdom), and biomass was quantified using the crystal violet assay, as previously described (59). In addition, biofilm composition was analyzed using propidium monoazide (PMA) quantitative PCR (qPCR), a method able to differentiate live cells from a population (60). Samples were prepared as previously described (60), before sonication in 1 ml of PBS at 35 kHz for 10 min in an ultrasonic water bath to remove and disaggregate the biofilm (61). After sonication, samples were incubated in the dark with 50 μM PMA (Cambridge BioScience, Cambridge, United Kingdom) for 10 min to allow uptake of the dye. All samples were then exposed for 5 min to a 650-W halogen light before DNA was extracted using the QIAamp DNA minikit, per the manufacturer's protocol (Qiagen, Crawley, United Kingdom). One microliter of extracted DNA was then added to a master mix containing Fast SYBR Green master mix, RNase-free water, and 10 μM *C. auris*-specific forward and reverse primers (forward, CGCACATTGCGCCTTGGGGTA; reverse, GTAGTCCTACCTGATTTGAGGCGAC) (62). Real-time qPCR was then used to enumerate the total of number of live cells from within the biofilm, using the following thermal profile: 50°C for 2 min and 95°C for 2 min, followed by 40 cycles of 95°C for 3 s and 60°C for 30 s. Colony-forming equivalents (CFE) were then calculated based upon a standard curve of serially extracted DNA ranging from 1×10^8 to 1×10^4 cells/ml.

Biofilm visualization. Biofilms were standardized and grown on Thermanox coverslips (Fisher Scientific, Loughborough, United Kingdom) as described above. At selected time points, biofilms were washed with PBS before processing for scanning electron microscopy (SEM). Biofilms were fixed in 2% paraformaldehyde, 2% glutaraldehyde, 0.15 M sodium cacodylate, and 0.15% (wt/vol) alcian blue, before being processed as previously described (59). Biofilms were then sputter coated in gold before being viewed under a JEOL-JSM-6400 microscope.

Planktonic and sessile susceptibility testing. Planktonic MICs (pMICs) were determined visually using the Clinical and Laboratory Standards Institute M27-A3 broth microdilution method (63). Standardized cells were treated with serial 2-fold dilutions of miconazole nitrate (0.25 to 128 mg/liter), micafungin (0.25 to 128 mg/liter), and amphotericin B (0.063 to 32 mg/liter). In addition, biofilms were grown for 4, 12, and 24 h as described above before treatment with the same concentrations as planktonic cells. Sessile MICs (sMICs) were determined using the XTT [2,3-bis(2-methoxy-4-nitro-5-sulfophenyl)-2H-tetrazolium-5-carboxanilide salt] metabolic reduction assay (64). The sMIC was calculated as the concentration leading to 80% reduction in XTT colorimetric readings in comparison to an untreated positive control.

RNA extraction and sequencing analysis. Following biofilm characterization, *C. auris* NCPF8973, originally isolated from a wound swab (14), was chosen for subsequent transcriptomic analysis. Biofilms were grown as described above in 75-cm³ tissue culture flasks before being washed with PBS, and biomass was dislodged using a cell scraper. The resultant biofilm biomass was then homogenized using

a bead beater, and RNA was extracted using the Trizol (Life Technologies, Paisley, United Kingdom) method (65). Following extraction, RNA was DNase treated and purified using the RNeasy MinElute cleanup kit per the manufacturer's instructions. Quality and quantity were assessed using a Bioanalyzer (Agilent, USA), where a minimum quantity of 2.5 μg and a minimum-quality RNA integrity number (RIN) value of 7.0 were obtained for each sample. Samples were then submitted to Edinburgh Genomics (<http://genomics.ed.ac.uk/>) before sequencing using the HiSeq 2500 Illumina sequencer. Biological triplicates were analyzed for all variables, with the exception of 4-h biofilms, for which two replicates were used due to sequencing failure.

Transcriptome annotation and differential expression analysis. Raw fastq reads were quality controlled using Trim Galore v0.4.5 (<https://github.com/FelixKrueger/TrimGalore>) to remove Illumina adapters and trim reads with a quality score lower than 20. Reads were then aligned to the RefSeq genome sequence B8441 using HISAT2 (66). The aligned reads were then coordinate sorted, and SAM files were converted to BAM before all aligned reads were merged using SAMtools (38). The resulting aligned reads were assembled *de novo* using genome-guided Trinity v2.5.1 (66). The completed transcriptome was assessed by using the contig length distribution metrics (N_{50}), percentage of annotation, and the third-party Benchmarking Universal Single-Copy Orthologs (BUSCO) v3 assessment program (<http://busco.ezlab.org/>). Annotation of candidate open reading frames (ORFs), identified with TransDecoder v5.0.2 (<http://transdecoder.sourceforge.net/>), was then performed using the Trinotate v3.1.0 package (<https://trinotate.github.io/>). Trinotate performs functional annotation of transcriptomes from the UniProt Swiss-Prot database via homology searches with the Basic Local Alignment Search Tool (BLAST) functions BLASTp for protein queries and BLASTx for nucleotide queries. Gene Ontology (GO) and Kyoto Encyclopedia of Genes and Genomes (KEGG) EggNOG identifiers were also inferred from the Swiss-Prot protein database. BLAST2GO annotation was additionally performed, which also relies upon BLAST but includes the annotation from European Bioinformatics Institute (EBI) InterPro databases. The extraction through to the annotation is summarized in Fig. 2. The reference transcriptome created by Trinity was used to create an index, and the trimmed reads were then counted and annotated against this index using Kallisto gene abundance quantification software. Gene abundance files for each sample replicate were then imported into R for differential analysis based upon the DESeq2 package. All additional statistics, analysis, and visualization were produced within R.

Temporal efflux pump activity and inhibition. The efflux pump activity of planktonic and sessile cells was assessed using the alanine β -naphthylamine (Ala-Nap) fluorescent assay as previously described (38). For planktonic assessment, four *C. auris* isolates were standardized to 5×10^7 cells/ml in the assay buffer solution (MgSO_4 [1 mM], K_2HPO_4 [50 mM], and 0.4% glucose, pH 7.0). For sessile cells, biofilms were grown in black flat-bottomed microtiter plates for 12 and 24 h. Following biofilm development, these were washed with the assay buffer solution. The reaction was then initiated with the addition of 100 $\mu\text{g}/\text{ml}$ Ala-Nap and developed for 60 min at 37°C. Fluorescence readings were obtained every 30 s using a fluorescence plate reader at an emission/excitation wavelength of 355/460 nm. In addition, the efflux pump inhibitor (EPI; L-Phe-L-Arg- β -naphthylamine dihydrochloride) was used in combination with fluconazole to determine if antifungal activity could be enhanced. Biofilms were developed in the presence of fluconazole (128 to 0.25 mg/liter) with and without the presence of EPI at a concentration of 64 mg/liter and incubated for 12 and 24 h at 37°C. Biofilms were then washed with PBS, before viability was calculated using the XTT assay as described above.

Statistical analysis. Graph production, data distribution, and statistical analysis were carried out using GraphPad Prism (version 8; La Jolla, CA) and R Studio (version 1.1). For efflux pump activity experiments, data were normalized before Student's *t* test was used to compare samples. Statistical significance was achieved if *P* was <0.05.

Data availability. Raw data files are deposited under accession no. PRJNA477447.

SUPPLEMENTAL MATERIAL

Supplemental material for this article may be found at <https://doi.org/10.1128/mSphere.00334-18>.

FIG S1, TIF file, 2.1 MB.

FIG S2, TIF file, 2.1 MB.

FIG S3, TIF file, 2.1 MB.

FIG S4, TIF file, 2.1 MB.

DATA SET S1, XLSX file, 12 MB.

DATA SET S2, XLSX file, 0.3 MB.

ACKNOWLEDGMENTS

This study has been funded by a research grant in 2017 by the European Society of Clinical Microbiology and Infectious Diseases (ESCMID) to L.S. We acknowledge funding support of the BBSRC Industrial CASE PhD studentship for C.D. (BB/P504567/1).

We thank Jose Lopez-Ribot (University of Texas at San Antonio) for his useful insights and critique of the manuscript.

REFERENCES

- Bongomin F, Gago S, Oladele RO, Denning DW. 2017. Global and multi-national prevalence of fungal diseases—estimate precision. *J Fungi* 3(4):57. <https://doi.org/10.3390/jof3040057>.
- Jeffery-Smith A, Taori SK, Schelenz S, Jeffery K, Johnson EM, Borman A, *Candida auris* Incident Management Team, Manuel R, Brown CS. 2018. *Candida auris*: a review of the literature. *Clin Microbiol Rev* 31:e00029-17. <https://doi.org/10.1128/CMR.00029-17>.
- Calvo B, Melo AS, Perozo-Mena A, Hernandez M, Francisco EC, Hagen F, Meis JF, Colombo AL. 2016. First report of *Candida auris* in America: clinical and microbiological aspects of 18 episodes of candidemia. *J Infect* 73:369–374. <https://doi.org/10.1016/j.jinf.2016.07.008>.
- Lockhart SR, Etienne KA, Vallabhaneni S, Farooqi J, Chowdhary A, Govenender NP, Colombo AL, Calvo B, Cuomo CA, Desjardins CA, Berkow EL, Castanheira M, Magobo RE, Jabeen K, Asghar RJ, Meis JF, Jackson B, Chiller T, Litvintseva AP. 2017. Simultaneous emergence of multidrug-resistant *Candida auris* on 3 continents confirmed by whole-genome sequencing and epidemiological analyses. *Clin Infect Dis* 64:134–140. <https://doi.org/10.1093/cid/ciw691>.
- Ruiz-Gaitán A, Moret AM, Tasiias-Pitarch M, Aleixandre-López AI, Martínez-Morel H, Calabuig E, Salavert-Lleti M, Ramírez P, López-Hontangas JL, Hagen F, Meis JF, Mollar-Maseres J, Pemán J. 2018. An outbreak due to *Candida auris* with prolonged colonization and candidemia in a tertiary care European hospital. *Mycoses* <https://doi.org/10.1111/myc.12781>.
- Schelenz S, Hagen F, Rhodes JL, Abdolrasouli A, Chowdhary A, Hall A, Ryan L, Shackleton J, Trimlett R, Meis JF, Armstrong-James D, Fisher MC. 2016. First hospital outbreak of the globally emerging *Candida auris* in a European hospital. *Antimicrob Resist Infect Contr* 5:35. <https://doi.org/10.1186/s13756-016-0132-5>.
- Chowdhary A, Prakash A, Sharma C, Kordalewska M, Kumar A, Sarma S, Tarai B, Singh A, Upadhyaya G, Upadhyay S, Yadav P, Singh PK, Khillan V, Sachdeva N, Perlin DS, Meis JF. 2018. A multicentre study of antifungal susceptibility patterns among 350 *Candida auris* isolates (2009–17) in India: role of the ERG11 and FKS1 genes in azole and echinocandin resistance. *J Antimicrob Chemother* 73:891–899. <https://doi.org/10.1093/jac/dkx480>.
- Kordalewska M, Lee A, Park S, Berrío I, Chowdhary A, Zhao Y, Perlin DS. 2018. Understanding echinocandin resistance in the emerging pathogen *Candida auris*. *Antimicrob Agents Chemother* 62:e00238-18. <https://doi.org/10.1128/AAC.00238-18>.
- Rajendran R, Sherry L, Nile CJ, Sherriff A, Johnson EM, Hanson MF, Williams C, Munro CA, Jones BJ, Ramage G. 2016. Biofilm formation is a risk factor for mortality in patients with *Candida albicans* bloodstream infection—Scotland, 2012–2013. *Clin Microbiol Infect* 22:87–93. <https://doi.org/10.1016/j.cmi.2015.09.018>.
- Soldini S, Posteraro B, Vella A, De Carolis E, Borghi E, Falleni M, Losito AR, Maiuro G, Trecarichi EM, Sanguinetti M, Tumbarello M. 2017. Microbiologic and clinical characteristics of biofilm-forming *Candida parapsilosis* isolates associated with fungaemia and their impact on mortality. *Clin Microbiol Infect* 24:771–777. <https://doi.org/10.1016/j.cmi.2017.11.005>.
- Tumbarello M, Fiori B, Trecarichi EM, Posteraro P, Losito AR, De Luca A, Sanguinetti M, Fadda G, Cauda R, Posteraro B. 2012. Risk factors and outcomes of candidemia caused by biofilm-forming isolates in a tertiary care hospital. *PLoS One* 7:e33705. <https://doi.org/10.1371/journal.pone.0033705>.
- Kean R, Delaney C, Rajendran R, Sherry L, Metcalfe R, Thomas R, McLean W, Williams C, Ramage G. 2018. Gaining insights from *Candida* biofilm heterogeneity: one size does not fit all. *J Fungi* 4(1):12. <https://doi.org/10.3390/jof4010012>.
- Rodrigues CF, Rodrigues ME, Silva S, Henriques M. 2017. *Candida glabrata* biofilms: how far have we come? *J Fungi* 3(1):11. <https://doi.org/10.3390/jof3010011>.
- Borman AM, Szekely A, Johnson EM. 2016. Comparative pathogenicity of United Kingdom isolates of the emerging pathogen *Candida auris* and other key pathogenic *Candida* species. *mSphere* 1:e00189-16. <https://doi.org/10.1128/mSphere.00189-16>.
- Ben-Ami R, Berman J, Novikov A, Bash E, Shachor-Meyouhas Y, Zakin S, Maor Y, Tarabia J, Schechner V, Adler A, Finn T. 2017. Multidrug-resistant *Candida haemulonii* and *C. auris*, Tel Aviv, Israel. *Emerg Infect Dis* 23:195–203. <https://doi.org/10.3201/eid2302.161486>.
- Sherry L, Ramage G, Kean R, Borman A, Johnson EM, Richardson MD, Rautemaa-Richardson R. 2017. Biofilm-forming capability of highly virulent, multidrug-resistant *Candida auris*. *Emerg Infect Dis* 23:328–331. <https://doi.org/10.3201/eid2302.161320>.
- Chatterjee S, Alampalli SV, Nageshan RK, Chettiar ST, Joshi S, Tatu US. 2015. Draft genome of a commonly misdiagnosed multidrug resistant pathogen *Candida auris*. *BMC Genomics* 16:686. <https://doi.org/10.1186/s12864-015-1863-z>.
- Muñoz JF, Gade L, Chow NA, Loparev VN, Juieng P, Farrer RA, Litvintseva AP, Cuomo CA. 2018. Genomic basis of multidrug-resistance, mating, and virulence in *Candida auris* and related emerging species. *bioRxiv* <https://doi.org/10.1101/299917>.
- Ramage G, Robertson SN, Williams C. 2014. Strength in numbers: antifungal strategies against fungal biofilms. *Int J Antimicrob Agents* 43:114–120. <https://doi.org/10.1016/j.ijantimicag.2013.10.023>.
- Hunter S, Apweiler R, Attwood TK, Bairoch A, Bateman A, Binns D, Bork P, Das U, Daugherty L, Duquenne L, Finn RD, Gough J, Haft D, Hulo N, Kahn D, Kelly E, Laugraud A, Letunic I, Lonsdale D, Lopez R, Madera M, Maslen J, McAnulla C, McDowall J, Mistry J, Mitchell A, Mulder N, Natale D, Orengo C, Quinn AF, Selengut JD, Sigrist CJ, Thimma M, Thomas PD, Valentin F, Wilson D, Wu CH, Yeats C. 2009. InterPro: the integrative protein signature database. *Nucleic Acids Res* 37:D211–D215. <https://doi.org/10.1093/nar/gkn785>.
- Kean R, McCloud E, Townsend EM, Sherry L, Delaney C, Jones BL, Williams C, Ramage G. 2018. The comparative efficacy of antiseptics against *Candida auris* biofilms. *Int J Antimicrob Agents* <https://doi.org/10.1016/j.ijantimicag.2018.05.007>.
- Kean R, Sherry L, Townsend E, McCloud E, Short B, Akinbobola A, Mackay WG, Williams C, Jones BL, Ramage G. 2018. Surface disinfection challenges for *Candida auris*: an in-vitro study. *J Hosp Infect* 98:433–436. <https://doi.org/10.1016/j.jhin.2017.11.015>.
- Fu Y, Luo G, Spellberg BJ, Edwards JE, Jr, Ibrahim AS. 2008. Gene overexpression/suppression analysis of candidate virulence factors of *Candida albicans*. *Eukaryot Cell* 7:483–492. <https://doi.org/10.1128/EC.00445-07>.
- Martínez JP, Blanes R, Casanova M, Valentin E, Murgui A, Domínguez Á. 2016. Null mutants of *Candida albicans* for cell-wall-related genes form fragile biofilms that display an almost identical extracellular matrix proteome. *FEMS Yeast Res* 16:fow075. <https://doi.org/10.1093/femsyr/fow075>.
- Naglik JR, Moyes DL, Wächtler B, Hube B. 2011. *Candida albicans* interactions with epithelial cells and mucosal immunity. *Microbes Infect* 13:963–976. <https://doi.org/10.1016/j.micinf.2011.06.009>.
- Fox EP, Bui CK, Nett JE, Hartooni N, Mui MC, Andes DR, Nobile CJ, Johnson AD. 2015. An expanded regulatory network temporally controls *Candida albicans* biofilm formation. *Mol Microbiol* 96:1226–1239. <https://doi.org/10.1111/mmi.13002>.
- Kempf M, Cottin J, Licznar P, Lefrançois C, Robert R, Apsaire-Marchais V. 2009. Disruption of the GPI protein-encoding gene IFF4 of *Candida albicans* results in decreased adherence and virulence. *Mycopathologia* 168:73–77. <https://doi.org/10.1007/s11046-009-9201-0>.
- Liu Y, Filler SG. 2011. *Candida albicans* Als3, a multifunctional adhesin and invasin. *Eukaryot Cell* 10:168–173. <https://doi.org/10.1128/EC.00279-10>.
- Zhao X, Daniels KJ, Oh SH, Green CB, Yeater KM, Soll DR, Hoyer LL. 2006. *Candida albicans* Als3p is required for wild-type biofilm formation on silicone elastomer surfaces. *Microbiology* 152:2287–2299. <https://doi.org/10.1099/mic.0.28959-0>.
- Naglik JR, Moyes D, Makwana J, Kanzaria P, Tschlaski E, Weindl G, Tappuni AR, Rodgers CA, Woodman AJ, Challacombe SJ, Schaller M, Hube B. 2008. Quantitative expression of the *Candida albicans* secreted aspartyl proteinase gene family in human oral and vaginal candidiasis. *Microbiology* 154:3266–3280. <https://doi.org/10.1099/mic.0.2008/022293-0>.
- Nailis H, Kuchariková S, Ricicová M, Van Dijck P, Deforce D, Nelis H, Coenye T. 2010. Real-time PCR expression profiling of genes encoding potential virulence factors in *Candida albicans* biofilms: identification of model-dependent and -independent gene expression. *BMC Microbiol* 10:114. <https://doi.org/10.1186/1471-2180-10-114>.
- Winter MB, Salcedo EC, Lohse MB, Hartooni N, Gulati M, Sanchez H, Takagi J, Hube B, Andes DR, Johnson AD, Craik CS, Nobile CJ. 2016.

- Global identification of biofilm-specific proteolysis in *Candida albicans*. *mBio* 7:e01514-16. <https://doi.org/10.1128/mBio.01514-16>.
33. Taff HT, Mitchell KF, Edward JA, Andes DR. 2013. Mechanisms of *Candida* biofilm drug resistance. *Future Microbiol* 8:1325–1337. <https://doi.org/10.2217/fmb.13.101>.
 34. Bizerra FC, Nakamura CV, de Poersch C, Estivalet Svidzinski TI, Borsato Quesada RM, Goldenberg S, Krieger MA, Yamada-Ogatta SF. 2008. Characteristics of biofilm formation by *Candida tropicalis* and antifungal resistance. *FEMS Yeast Res* 8:442–450. <https://doi.org/10.1111/j.1567-1364.2007.00347.x>.
 35. Fonseca E, Silva S, Rodrigues CF, Alves CT, Azeredo J, Henriques M. 2014. Effects of fluconazole on *Candida glabrata* biofilms and its relationship with ABC transporter gene expression. *Biofouling* 30:447–457. <https://doi.org/10.1080/08927014.2014.886108>.
 36. Mukherjee PK, Chandra J, Kuhn DM, Ghannoum MA. 2003. Mechanism of fluconazole resistance in *Candida albicans* biofilms: phase-specific role of efflux pumps and membrane sterols. *Infect Immun* 71:4333–4340. <https://doi.org/10.1128/IAI.71.8.4333-4340.2003>.
 37. Ramage G, Bachmann S, Patterson TF, Wickes BL, López-Ribot JL. 2002. Investigation of multidrug efflux pumps in relation to fluconazole resistance in *Candida albicans* biofilms. *J Antimicrob Chemother* 49:973–980. <https://doi.org/10.1093/jac/dk049>.
 38. Rajendran R, Mowat E, McCulloch E, Lappin DF, Jones B, Lang S, Majithiya JB, Warn P, Williams C, Ramage G. 2011. Azole resistance of *Aspergillus fumigatus* biofilms is partly associated with efflux pump activity. *Antimicrob Agents Chemother* 55:2092–2097. <https://doi.org/10.1128/AAC.01189-10>.
 39. Liu TT, Lee RE, Barker KS, Lee RE, Wei L, Homayouni R, Rogers PD. 2005. Genome-wide expression profiling of the response to azole, polyene, echinocandin, and pyrimidine antifungal agents in *Candida albicans*. *Antimicrob Agents Chemother* 49:2226–2236. <https://doi.org/10.1128/AAC.49.6.2226-2236.2005>.
 40. Pierce CG, Vila T, Romo JA, Montelongo-Jauregui D, Wall G, Ramasubramanian A, Lopez-Ribot JL. 2017. The *Candida albicans* biofilm matrix: composition, structure and function. *J Fungi* 3(1):14. <https://doi.org/10.3390/jof3010014>.
 41. Dominguez E, Zarnowski R, Sanchez H, Covelli AS, Westler WM, Azadi P, Nett J, Mitchell AP, Andes DR. 2018. Conservation and divergence in the *Candida* species biofilm matrix mannan-glucan complex structure, function, and genetic control. *mBio* 9:e00451-18. <https://doi.org/10.1128/mBio.00451-18>.
 42. Silva S, Henriques M, Martins A, Oliveira R, Williams D, Azeredo J. 2009. Biofilms of non-*Candida albicans* *Candida* species: quantification, structure and matrix composition. *Med Mycol* 47:681–689. <https://doi.org/10.3109/13693780802549594>.
 43. Lohse MB, Gulati M, Johnson AD, Nobile CJ. 2018. Development and regulation of single- and multi-species *Candida albicans* biofilms. *Nat Rev Microbiol* 16:19–31. <https://doi.org/10.1038/nrmicro.2017.107>.
 44. Taff HT, Nett JE, Zarnowski R, Ross KM, Sanchez H, Cain MT, Hamaker J, Mitchell AP, Andes DR. 2012. A *Candida* biofilm-induced pathway for matrix glucan delivery: implications for drug resistance. *PLoS Pathog* 8:e1002848. <https://doi.org/10.1371/journal.ppat.1002848>.
 45. Zarnowski R, Westler WM, Lacmbouh GA, Marita JM, Bothe JR, Bernhardt J, Lounes-Hadj Sahraoui A, Fontaine J, Sanchez H, Hatfield RD, Ntambi JM, Nett JE, Mitchell AP, Andes DR. 2014. Novel entries in a fungal biofilm matrix encyclopedia. *mBio* 5:e01333-14. <https://doi.org/10.1128/mBio.01333-14>.
 46. Fisher MC, Hawkins NJ, Sanglard D, Gurr SJ. 2018. Worldwide emergence of resistance to antifungal drugs challenges human health and food security. *Science* 360:739–742. <https://doi.org/10.1126/science.aap7999>.
 47. Denning DW, Bromley MJ. 2015. Infectious disease. How to bolster the antifungal pipeline. *Science* 347:1414–1416. <https://doi.org/10.1126/science.aaa6097>.
 48. Perfect JR. 2017. The antifungal pipeline: a reality check. *Nat Rev Drug Discov* 16:603–616. <https://doi.org/10.1038/nrd.2017.46>.
 49. Berkow EL, Angulo D, Lockhart SR. 2017. *In vitro* activity of a novel glucan synthase inhibitor, SCY-078, against clinical isolates of *Candida auris*. *Antimicrob Agents Chemother* 61:e00435-17. <https://doi.org/10.1128/AAC.00435-17>.
 50. Berkow EL, Lockhart SR. 2018. Activity of CD101, a long-acting echinocandin, against clinical isolates of *Candida auris*. *Diagn Microbiol Infect Dis* 90:196–197. <https://doi.org/10.1016/j.diagmicrobio.2017.10.021>.
 51. Hager CL, Larkin EL, Long L, Zohra Abidi F, Shaw KJ, Ghannoum MA. 2018. *In vitro* and *in vivo* evaluation of the antifungal activity of APX001A/APX001 against *Candida auris*. *Antimicrob Agents Chemother* 62:e02319-17. <https://doi.org/10.1128/AAC.02319-17>.
 52. Hashemi MM, Rovig J, Holden BS, Taylor MF, Weber S, Wilson J, Hilton B, Zaugg AL, Ellis SW, Yost CD, Finnegan PM, Kistler CK, Berkow EL, Deng S, Lockhart SR, Peterson M, Savage PB. 2018. Ceragenins are active against drug-resistant *Candida auris* clinical isolates in planktonic and biofilm forms. *J Antimicrob Chemother* 73:1537–1545. <https://doi.org/10.1093/jac/dky085>.
 53. Zhao M, Lepak AJ, VanScoy B, Bader JC, Marchillo K, Vanhecker J, Ambrose PG, Andes DR. 2018. *In vivo* pharmacokinetics and pharmacodynamics of APX001 against *Candida* spp. in a neutropenic disseminated candidiasis mouse model. *Antimicrob Agents Chemother* 62:e02542-17. <https://doi.org/10.1128/AAC.02542-17>.
 54. Larkin E, Hager C, Chandra J, Mukherjee PK, Retuerto M, Salem I, Long L, Ishano N, Kovanda L, Borroto-Esoda K, Wring S, Angulo D, Ghannoum M. 2017. The emerging pathogen *Candida auris*: growth phenotype, virulence factors, activity of antifungals, and effect of SCY-078, a novel glucan synthesis inhibitor, on growth morphology and biofilm formation. *Antimicrob Agents Chemother* 61:e02396-16. <https://doi.org/10.1128/AAC.02396-16>.
 55. Grahl N, Demers EG, Crocker AW, Hogan DA. 2017. Use of RNA-protein complexes for genome editing in non-*albicans* *Candida* species. *mSphere* 2:e00218-17. <https://doi.org/10.1128/mSphere.00218-17>.
 56. Defosse TA, Le Govic Y, Vandeputte P, Courdavault V, Clastre M, Bouchara JP, Chowdhary A, Giglioli-Guivarc'h N, Papon N. 2018. A synthetic construct for genetic engineering of the emerging pathogenic yeast *Candida auris*. *Plasmid* 95:7–10. <https://doi.org/10.1016/j.plasmid.2017.11.001>.
 57. Nobile CJ, Fox EP, Nett JE, Sorrells TR, Mitrovich QM, Hernday AD, Tuch BB, Andes DR, Johnson AD. 2012. A recently evolved transcriptional network controls biofilm development in *Candida albicans*. *Cell* 148:126–138. <https://doi.org/10.1016/j.cell.2011.10.048>.
 58. Borman AM, Szekely A, Johnson EM. 2017. Isolates of the emerging pathogen *Candida auris* present in the UK have several geographic origins. *Med Mycol* 55:563–567. <https://doi.org/10.1093/mmy/myw147>.
 59. Kean R, Rajendran R, Haggarty J, Townsend EM, Short B, Burgess KE, Lang S, Millington O, Mackay WG, Williams C, Ramage G. 2017. *Candida albicans* mycofilms support *Staphylococcus aureus* colonization and enhances miconazole resistance in dual-species interactions. *Front Microbiol* 8:258. <https://doi.org/10.3389/fmicb.2017.00258>.
 60. Sherry L, Lappin G, O'Donnell LE, Millhouse E, Millington OR, Bradshaw DJ, Axe AS, Williams C, Nile CJ, Ramage G. 2016. Viable compositional analysis of an eleven species oral polymicrobial biofilm. *Front Microbiol* 7:912. <https://doi.org/10.3389/fmicb.2016.00912>.
 61. Tunney MM, Patrick S, Gorman SP, Nixon JR, Anderson N, Davis RI, Hanna D, Ramage G. 1998. Improved detection of infection in hip replacements. A currently underestimated problem. *J Bone Joint Surg Br* 80:568–572. <https://doi.org/10.1302/0301-620X.80B4.8473>.
 62. Kordalewska M, Zhao Y, Lockhart SR, Chowdhary A, Berrio I, Perlin DS. 2017. Rapid and accurate molecular identification of the emerging multidrug-resistant pathogen *Candida auris*. *J Clin Microbiol* 55:2445–2452. <https://doi.org/10.1128/JCM.00630-17>.
 63. CLSI. 2008. Reference method for broth dilution antifungal susceptibility testing of yeasts. Approved standard M27–A3, 3rd ed. CLSI, Wayne, PA.
 64. Ramage G, Vande Walle K, Wickes BL, López-Ribot JL. 2001. Standardized method for *in vitro* antifungal susceptibility testing of *Candida albicans* biofilms. *Antimicrob Agents Chemother* 45:2475–2479. <https://doi.org/10.1128/AAC.45.9.2475-2479.2001>.
 65. Rajendran R, May A, Sherry L, Kean R, Williams C, Jones BL, Burgess KV, Heringa J, Abeln S, Brandt BW, Munro CA, Ramage G. 2016. Integrating *Candida albicans* metabolism with biofilm heterogeneity by transcriptome mapping. *Sci Rep* 6:35436. <https://doi.org/10.1038/srep35436>.
 66. Haas BJ, Papanicolaou A, Yassour M, Grabherr M, Blood PD, Bowden J, Couger MB, Eccles D, Li B, Lieber M, MacManes MD, Ott M, Orvis J, Pochet N, Strozzi F, Weeks N, Westerman R, William T, Dewey CN, Henschel R, LeDuc RD, Friedman N, Regev A. 2013. De novo transcript sequence reconstruction from RNA-seq using the Trinity platform for reference generation and analysis. *Nat Protoc* 8:1494–1512. <https://doi.org/10.1038/nprot.2013.084>.